On the formation of small molecules by radiative assocation

Sergey V. Antipov

Thesis for the Degree of Doctor of Philosophy in Natural Science specializing in Chemistry. The thesis will be presented and defended on Monday March 18th, 2013, at 10:15 in room 10:an, Kemigården 4, Gothenburg.

Supervisor: Docent Magnus Gustafsson, University of Gothenburg

Assistant supervisor: Professor Gunnar Nyman, University of Gothenburg

Examiner: Professor Leif Eriksson, University of Gothenburg

Opponent: Professor David E. Manolopoulos, University of Oxford

UNIVERSITY OF GOTHENBURG
Gothenburg, Sweden 2013

ISBN 978-91-628-8650-9
Part I available at http://hdl.handle.net/2077/32195

Printed by Ale Tryckteam AB

Abstract

This thesis is devoted to the theoretical investigation of radiative association, which is one of the processes contributing to formation of molecules in the interstellar medium. The formation of the CN, SiN, SiP and CO molecules through radiative association of the corresponding atoms in their ground electronic states is studied by the means of classical and quantum dynamical calculations. In all cases the Born–Oppenheimer approximation is employed. The corresponding rate coefficients are calculated and the Breit–Wigner theory is used to properly account for the resonance contributions.

Some common features of the radiative association process for the considered systems are discovered. For example, a drop in magnitude of the cross sections at high energy and, consequently, the high-temperature rate coefficients is observed. Also, is is shown that in the absence of a potential barrier the semi-classical formalism provides a good estimate for the rate coefficients.

A pronounced isotope effect is discovered for the formation of CO by radiative association of C(^3P) and O(^3P) atoms. It is shown that the presence of a potential barrier on the $A^1\Pi$ electronic state of carbon monoxide leads to different formation channels for the ^{12}CO and ^{13}CO isotopologues at low temperatures.

The role of spin-orbit and rotational couplings in radiative association of C(^3P) and N(^4S) atoms is investigated. Couplings among doublet electronic states of the CN radical are considered, giving rise to a 6-state model of the process. Comparison of the energy-dependent rate coefficients calculated with and without spin-orbit and rotational couplings shows that these have a strong effect on the resonance structure and low-energy baseline of the rate coefficient.

Preface

The present thesis is composed of five research papers and an introductory part that serves to describe the theoretical approach to the problem and methods used in its solution. The following is a list of included papers referred to in the text by their Roman numerals:

I. **Rate coefficient of CN formation through radiative association: A theoretical study of quantum effects**
Sergey V. Antipov, Tobias Sjölander, Gunnar Nyman, and Magnus Gustafsson
J. Chem. Phys., **131**, 074302 (2009).

II. **Refined theoretical study of radiative association: Cross sections and rate constants for the formation of SiN**
Magnus Gustafsson, Sergey V. Antipov, Jan Franz, and Gunnar Nyman
J. Chem. Phys., **137**, 104301 (2012).

III. **Formation of the SiP radical through radiative association**
Nikolay V. Golubev, Dmirty S. Bezrukov, Magnus Gustafsson, Gunnar Nyman, and Sergey V. Antipov
Manuscript (2013).

IV. **Isotope effect in formation of carbon monoxide through radiative association**
Sergey V. Antipov, Magnus Gustafsson, and Gunnar Nyman
MNRAS, doi: 10.1093/mnras/sts615 (2013).

V. **Spin-orbit and rotational couplings in radiative association of C(^3P) and N(^4S) atoms**
Sergey V. Antipov, Magnus Gustafsson, and Gunnar Nyman
J. Chem. Phys., **135**, 184302 (2011).

Contribution from the author

The author took part in analysis and discussion of the results presented in the included papers.

I. The author performed the calculations of the quantum mechanical cross sections, the resonance parameters, the rate coefficients and wrote the manuscript.

II. The author proposed the use of the optical potential method and performed the calculations of the resonance parameters and the rate coefficients.

III. The author acted as principal supervisor for Nikolay V. Golubev, the visiting student working on the project; wrote the manuscript.

IV. The author did the calculations of the resonance parameters and the rate coefficients and wrote the manuscript.

V. The author carried out necessary mathematical derivations, performed all calculations and wrote the manuscript.

Acknowledgments

I am indebted to my supervisors Docent Magnus Gustafsson and Professor Gunnar Nyman for the invaluable support, encouragement, discussions and, what might be the most important, for their patience during the previous four and a half years. Once you decided to choose my application among the others. I hope that, would you be given another chance, you would do the same. Thank you.

I would like to express my gratitude to the examiners. To Prof. Sture Nordholm, who's wisdom and good advice helped me a lot during the earlier years of my PhD. To Prof. Leif Eriksson, who soon after his arrival at the department agreed to take on the duty and allowed me to progress along the chosen path.

During the summer of 2011, I spent some time as a researcher at the Institute of Theoretical Atomic Molecular and Optical Physics (ITAMP) at Cambridge, MA, USA. I would like to thank my host there Dr. James F. Babb for giving me an excellent opportunity to join such a stimulating research environment.

I want to thank all members, former and present, of the Physical Chemistry group. You made my time here pleasant and enjoyable.

I wish to express my gratitude to Master Andrew Ewing and all members of the Gothenburg Tang Soo Do club. All the fun we had at our training and Tang Soo Do coffee breaks or elsewhere will be remembered. Thanks for keeping me sane during the last year of my PhD studies. Ko Map Sum Ni Da and Tang Soo!

There are two persons whose advice helped me to decide my path, ultimately leading me to Sweden, and to whom I owe a lot. I thank Dr. Yaroslav A. Sakharov from the Polar Geophysical Institute of the Russian Academy of Science for constant motivation and encouragement to aim for the highest possible goal. Also, I am grateful to Dr. Ilya G. Ryabinkin, currently at the University of Toronto, for motivating me to pursue PhD studies abroad and for his invaluable help and support at the time I was looking for a position.

Last but not least, I thank my family for their constant support, love and care. This work would not have been possible without you.

Contents

Chapter 1

Introduction

> Every attempt to employ mathematical methods in the study of chemical questions must be considered profoundly irrational and contrary to the spirit of chemistry...
>
> Auguste Comte
> *Cours de philosophie positive*

Formation of molecules is one of the cornerstones of chemistry and understanding molecule formation in different environments is of central interest. Historically, the knowledge about chemical nature of various processes, formation and properties of new compounds would come from experimental studies and observations. Over the centuries great knowledge has been accumulated based solely on experimental studies.

However, with the rapid development of computers in late 20^{th} century theoretical simulations started to play a big role in natural science. Nowadays, large scale simulations of various chemical processes, which could range from the formation of a simple diatomic molecule to the structural re-arrangements in proteins due to reaction with some other molecule, are possible to perform. Such simulations together with experimental studies provide a much deeper insight into the nature of things than experiments alone. Moreover, theoretical calculations can be used to gain an insight into processes and systems, which are not accessible experimentally.

The present thesis is devoted to the theoretical investigation of radiative association, which is one of the processes contributing to formation of molecules in the interstellar medium. Experimental studies of such process

are very complicated and, thus, theoretical modeling becomes one of the few reliable ways to advance the understanding of radiative association.

In this thesis formation of some diatomic molecules such as CN, SiN, SiP and CO by radiative association is studied by the means of classical and quantum dynamical calculations. The thesis consists of two parts: an introductory part, which is followed by the included scientific articles, available only in the printed version. The rest of the introductory part is organized as follows. Chapter 2 gives an introduction to radiative association and discusses its relevance for astrochemistry. In Chapter 3 a theoretical description of the radiative association process is given. Chapter 4 summarizes quantum dynamical methods used in the work presented here. A summary of the main results and findings of this thesis can be found in Chapter 5 and conclusion and outlook are given in Chapter 6.

Chapter 2

Radiative association

2.1 General discussion

Radiative association is a two-body collisional process in which the collision of two species, A and B, is followed by spontaneous emission of a photon in order to stabilize the collision complex:

$$\mathrm{A} + \mathrm{B} \rightarrow \mathrm{AB}^* \rightarrow \mathrm{AB} + h\nu. \tag{2.1}$$

The process is schematically depicted in Fig. 2.1. In the simplest case, A and B are atoms, but they can also be neutral molecules or ions.

When relatively big molecules are involved, radiative association can be quite efficient and is believed to be important in the formation of polyatomic compounds in dense molecular clouds [1, 2]. On the contrary, radiative association of atoms or atomic ions is a slow process and usually the stabilization of the collisional complex AB^* will happen through the collision with a third body rather than by photon emission. Despite this, radiative association is still considered as one of the important mechanisms of molecule formation in dust-poor environments [3], where the densities are too low to allow for

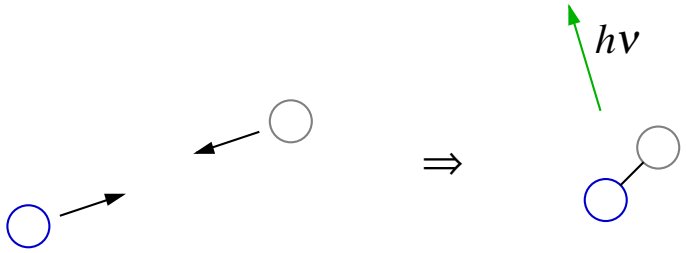

Figure 2.1: Schematic representation of radiative association.

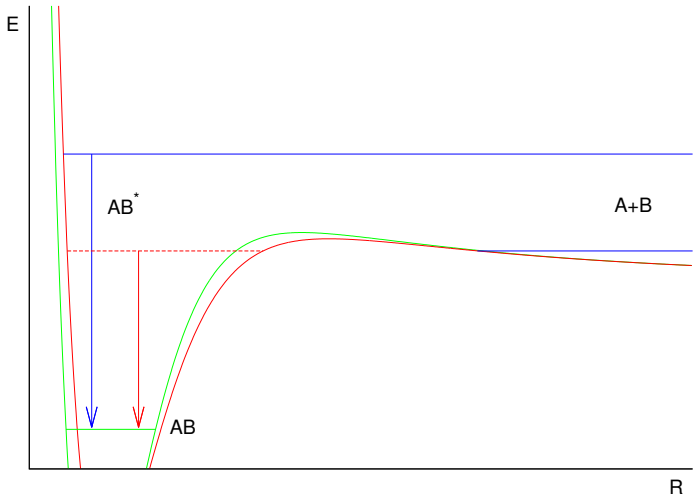

Figure 2.2: Schematic illustration of the direct (blue arrow) and resonant (red arrow) mechanisms of radiative association.

ternary collisions, and as a key step in the chemical evolution of protoplanetary disks [4]. In addition, formation of certain diatomic molecules through reaction (2.1) can play an important role in planetary atmospheres. For example, radiative association of N and O atoms is a significant source of emission in the terrestrial nightglow and in the atmosphere of Venus (see Ref. [5] and references therein).

Usually, two different mechanisms, which contribute to the formation of molecules by radiative association, are distinguished: resonant and direct (non-resonant) and both are shown in Fig. 2.2. The direct process occurs when the initial kinetic energy of the colliding particles is high enough to overcome any barrier (potential or centrifugal) on the initial electronic state and the spontaneous emission brings the system directly from the continuum to a bound level. The resonance contribution is due to the quantum mechanical tunneling through the barrier, in which case the colliding particles form a quasi-bound state. The latter can decay by the tunneling back through the barrier to reform reactants or undergo a radiative transition to a bound level leading to molecule formation.

Due to the astrochemical importance, formation of small molecules by radiative association attracts much of attention from researchers and the main interest is to obtain the rate coefficients of radiative association. As will be

discussed below (Sec. 2.2) experimental measurements of the rate constant for such processes is complicated and astronomers who investigate the chemical evolution in interstellar space can instead rely on computed radiative association rates. The semi-classical and quantum mechanical theories for such calculations have been worked out before, see e.g. the review by Babb and Kirby [3] and rate coefficients have been computed for some neutral [5–12] as well as a number of ionic systems [5, 11, 13–17].

2.2 Experimental studies

The experimental study of radiative association in a laboratory is quite complicated. At normal densities the process is obscured by ternary collisions and, thus, the experimental measurements of the radiative association rate coefficients should be done at low densities. Although very low densities can be attained experimentally, the probability of observing a single reaction product increases with the density and the sensitivity of the measurement becomes crucial. One possible solution is to use ion-trapping techniques in order to accumulate enough products. However, such an approach limits the class of system that can be studied [18].

Successful applications of the ion cyclotron resonance technique to measure the radiative association rate coefficient for reactions between polyatomic molecules have been reported [1]. However, this method allows to study reactions with the rate coefficient being of the order 10^{-10} cm^3/s or higher at room temperatures. Thus, it is not sensitive enough to allow for studies of radiative association of small molecules. Up to date only a few experimental works based on the use of ion traps for the direct measurements of the radiative association rate constant for formation of small molecules are available in the literature [18–20].

Chapter 3

Theory

I soon realized that the part of chemistry I liked was called physics.

Isidor Isaac Rabi

In this chapter an overview of theoretical methods and approaches used to model the radiative association process is presented. The focus of this thesis is on the formation of small molecules and, thus, the description of different kinetics models used for radiative association of poly-atomic molecules [1, 21, 22] is not included.

3.1 Cross sections

The radiative association cross section can be calculated by a variety of approaches based on classical or quantum dynamics for the description of the nuclear motion. In this thesis three methods, viz. the perturbation theory (PT), optical potential (OP) and semi-classical (SC) approaches, are applied to study radiative association and the outline of those is given below.

3.1.1 Perturbation theory (PT) approach

A common theoretical treatment of radiative association is based on the dipole approximation for the interactions between the electric field and molecular system and thermodynamical relations for the Einstein A coefficient describing the spontaneous emission of a photon.[1] Under such approximations

[1] Derivations of both dipole approximation and Einstein A coefficient can be found in many standard quantum mechanics textbooks, see e.g. [23].

Table 3.1: Notations of quantum numbers.

L_{X}	Electronic orbital angular momentum of atom X
L	Total electronic orbital angular momentum of the diatomic system: $\vec{L} = \vec{L}_{\mathrm{A}} + \vec{L}_{\mathrm{B}}$
S_{X}	Electronic spin of atom X
S	Total electronic spin of the diatomic system: $\vec{S} = \vec{S}_{\mathrm{A}} + \vec{S}_{\mathrm{B}}$
l	Rotational angular momentum of the nuclei
J	Total angular momentum of the diatomic system: $\vec{J} = \vec{L} + \vec{S} + \vec{l}$
Λ	Projection of L on the internuclear axis
M	Projection of J on the space-fixed z-axis
v	Vibrational quantum number

the radiative association cross section is given by the Fermi Golden Rule-type formula (Paper V):

$$\sigma_n(E) = \sum_{J,v',J'} \frac{64}{3} \frac{\pi^5}{(4\pi\epsilon_0)k^2} \frac{P_n}{\lambda^3_{nEv'J'}} \sum_{M,M'} |\langle \Psi_{nJME} | \hat{\mathrm{D}} | \Psi_{J'M'v'} \rangle|^2, \tag{3.1}$$

where E is the kinetic energy of the colliding particles, $k = \frac{\sqrt{2\mu E}}{\hbar}$ is the wavenumber for the initial channel n, P_n is the statistical weight factor for approaching through the channel n, $\lambda_{nEv'J'}$ is the wavelength of the emitted photon, $\hat{\mathrm{D}}$ is the dipole moment operator and Ψ_{nJME} and $\Psi_{J'M'v'}$ are the continuum wavefunction of the initial state and the final rovibrational wavefunction, respectively. Notations for the quantum numbers used in this chapter are listed in Table 3.1.

In Eq. (3.1) no assumptions are made about the structure of the wavefunctions. However, the majority of publications, which use the PT approach to study formation of diatomic molecules through radiative association, rely on the Born–Oppenheimer (BO) approximation (see e.g. [3, 7, 9–11, 13, 17, 24–26]). The total wavefunctions are expressed as a product

$$\Psi_{nJMq} = \psi_{\Lambda SJq} |JM\rangle |\Lambda S\rangle, \tag{3.2}$$

where $\psi_{\Lambda SJq}$ is the radial wavefunction, and $|JM\rangle$ and $|\Lambda S\rangle$ are the rotational and electronic wavefunctions, respectively. Here q stands for the energy E for the continuum states and for the vibrational quantum number v, if the state is bound; index n is substituted by the quantum numbers characterizing a particular electronic state ΛS. In practice the BO approximation means that all couplings between different electronic states of the systems are neglected and only the radiative transitions due to spontaneous emission are allowed.

Thus, it allows us to study radiative association from the continuum of the initial electronic state ΛS to the bound levels of the final electronic state $\Lambda' S$[2].

Expansion (3.2) allows to factorize the matrix element of the dipole operator in Eq. (3.1) in the following form:

$$\sum_{M,M'} |\langle \Psi_{nJME} | \hat{\mathrm{D}} | \Psi_{J'M'v'} \rangle|^2 = \\ = S_{\Lambda S J \Lambda' S J'} |\langle \psi_{\Lambda S J E} | D_{\Lambda S \Lambda' S}(R) | \psi_{\Lambda' S J' v'} \rangle|^2, \qquad (3.3)$$

where the summation over M, M' and integration over rotational and electronic coordinates are carried out to give the matrix element of the dipole operator $D_{\Lambda S \Lambda' S'}(R)$ and the Hönl–London factors $S_{\Lambda S J \Lambda' S J'}$ [27, 28]. Substitution of Eq. (3.3) into Eq. (3.1) yields

$$\sigma_{\Lambda S \to \Lambda' S}(E) = \sum_{J v' J'} \frac{64}{3} \frac{\pi^5}{4\pi\epsilon_0} \frac{P_{\Lambda S}}{k^2} \frac{S_{\Lambda S J \Lambda' S J'}}{\lambda^3_{E \Lambda' S v' J'}} \times \\ \times \left| \langle \psi_{\Lambda S J E} | D_{\Lambda S \Lambda' S}(R) | \psi_{\Lambda' S J' v'} \rangle \right|^2. \qquad (3.4)$$

Unless stated otherwise, for the rest of the introductory part of the thesis it is assumed that the BO approximation is used and Eq. (3.4) is valid.

The PT approach in form of Eq. (3.4) was applied to model radiative association in Papers I-IV and in Paper V perturbation theory is used to study the role of spin-orbit and rotational couplings in radiative association of C(^3P) and N(^4S) atoms.

3.1.2 Optical potential (OP) method

Addition of a negative imaginary potential to the Hamiltonian operator causes loss of incident flux, which mimics the decay of the system through some process. Thus, the general idea of the explicit optical potential method is to modify the Hamiltonian operator in such a way that the loss of flux corresponds to the radiative decay due to spontaneous emission. Zygelman and Dalgarno [29] showed that the appropriate optical potential can be written as

$$V_{\mathrm{opt}}(R) = -\frac{i\hbar}{2} A_{\Lambda S \to \Lambda' S}(R), \qquad (3.5)$$

where

$$A_{\Lambda S \to \Lambda' S'}(R) = \frac{64}{3} \frac{\pi^4}{(4\pi\epsilon_0)h} \left(\frac{2 - \delta_{0,\Lambda+\Lambda'}}{2 - \delta_{0,\Lambda}} \right) \frac{D^2_{\Lambda S \Lambda' S}(R)}{\lambda^3_{\Lambda S \to \Lambda' S}(R)} \qquad (3.6)$$

[2]Since the dipole transitions between states of different multiplicity are forbidden $S' = S$.

is the semi-classical transition rate of spontaneous emission. In Eq. (3.6) $\lambda_{\Lambda S\to\Lambda' S}(R)$ is the optimal wavelength of the emitted photon:

$$\frac{1}{\lambda_{\Lambda S\to\Lambda' S}(R)} = \max\left(0, \frac{V_{\Lambda S}(R) - V_{\Lambda' S}(R)}{hc}\right). \tag{3.7}$$

The optical potential of the form (3.5) was applied before to study other radiative processes such as quenching [29], charge transfer [30] and electron capture[31].

Derivation of Eqs. (3.5)-(3.7) uses the completeness of the final states. It means that the defined transition rate describes spontaneous emission to both bound (radiative association) and continuum states (radiative quenching). In order to ensure that only radiative association is taken into account the restricted transition rate is defined

$$A^{EJ}_{\Lambda S\to\Lambda' S}(R) = \begin{cases} A_{\Lambda S\to\Lambda' S}(R) & V_{\Lambda' S}(R) + \frac{\hbar^2 J(J+1)}{2\mu R^2} < 0 \cup \\ & E < V_{\Lambda S}(R) - V_{\Lambda' S}(R) \\ 0 & \text{otherwise,} \end{cases} \tag{3.8}$$

where the first condition checks that the final effective potential may support bound states and the second that the initial kinetic energy of the system is below the optimal energy of the emitted photon, i.e. a vertical transition to the bound region is possible. The centrifugal term in the final effective potential is approximate ($J'\approx J$ and $\Lambda'\approx 0$), but the corresponding conditions mostly important for large J, which justifies the approximation.

Within the OP method the radiative association cross section is determined by

$$\sigma_{\Lambda S\to\Lambda' S}(E) = \frac{\pi\hbar^2}{2\mu E} P_{\Lambda S} \sum_J (2J+1)(1 - e^{-4\eta^{EJ}_{\Lambda S\to\Lambda' S'}}) \tag{3.9}$$

where $\eta^{EJ}_{\Lambda S\to\Lambda' S}$ is the imaginary part of the phase shift of the radial wavefunction $\psi^{EJ}_{\Lambda S\to\Lambda' S}(R)$, which obeys the the Schrödinger equation with the optical potential

$$\left(-\frac{\hbar^2}{2\mu}\frac{d^2}{dR^2} + \frac{\hbar^2(J(J+1)-\Lambda^2)}{2\mu R^2} + V_{\Lambda S}(R) - \frac{i}{2}A^{EJ}_{\Lambda S\to\Lambda' S}(R) - E\right)\psi^{EJ}_{\Lambda S\to\Lambda' S}(R) = 0. \tag{3.10}$$

From Eqs. (3.9) and (3.10) it is clear, that the presented implementation of the OP method does not require knowledge of the bound states of the

system. It makes this approach computationally more effective than PT. However, for exactly the same reason the presented method does not allow calculation of the radiative association emission spectrum. Further details, about theory, limitations and performance of the method are given in Paper II.

3.1.3 Semi-classical (SC) formalism

The semi-classical expression for the radiative association cross section can be derived from Eq. (3.9) by applying the distorted wave and JWKB approximations [29]. The resulting cross section is given by

$$\begin{aligned}\sigma_{\Lambda S\to\Lambda' S}(E) &= 4\pi\left(\frac{\mu}{2E}\right)^{1/2} P_{\Lambda S} \\ &\times \int_0^\infty b \int_{R_c}^\infty \frac{A^{Eb}_{\Lambda S\to\Lambda' S}(R) dR db}{(1 - V_{\Lambda S}(R)/E - b^2/R^2)^{1/2}},\end{aligned} \tag{3.11}$$

where R_c is the classical turning point (distance of closest approach) for the corresponding value of the impact parameter b and the restricted transition rate is defined in the same way as in Sec. (3.1.2), namely

$$A^{Eb}_{\Lambda S\to\Lambda' S}(R) = \begin{cases} A_{\Lambda S\to\Lambda' S}(R) & V_{\Lambda' S}(R) + \frac{Eb^2}{R^2} < 0 \cup \\ & E < V_{\Lambda S}(R) - V_{\Lambda' S}(R) \\ 0 & \text{otherwise.} \end{cases} \tag{3.12}$$

Here the classical expression for the rotational kinetic energy is used.

It should be mentioned that originally the semi-classical formula for the cross section (3.11) based on the unrestricted transition rate (3.6) was derived by Bates [32] using arguments of classical mechanics.

Within the present thesis the SC formalism was applied to study formation of CN (Paper I), SiN (Paper II), SiP (Paper III) and CO (Paper IV) through radiative association.

3.2 Rate coefficients

When the cross section for a collisional process such as radiative association is obtained, the rate coefficient at a temperature T can be calculated using the general expression

$$k_{\Lambda S\to\Lambda' S}(T) = \int_0^\infty v(E) W(E,T) \sigma_{\Lambda S\to\Lambda' S}(E) dE, \tag{3.13}$$

where

$$v(E) = \sqrt{\frac{2E}{\mu}}$$

is the relative velocity of colliding particles and $W(E,T)$ is the normalized energy distribution. Assuming that the system is in thermodynamic equilibrium, i.e. the Maxwell–Boltzmann distribution of energies,

$$W(E,T) = 2\sqrt{\frac{E}{\pi(k_\mathrm{B}T)^3}}e^{-E/k_\mathrm{B}T},$$

the rate coefficient is defined by

$$k_{\Lambda S\to\Lambda' S}(T) = \left(\frac{8}{\pi\mu}\right)^{1/2}\left(\frac{1}{k_\mathrm{B}T}\right)^{3/2}\int_0^\infty E\sigma_{\Lambda S\to\Lambda' S}(E)e^{-E/k_\mathrm{B}T}dE, \quad (3.14)$$

where k_B is the Boltzmann constant.

Let us consider practical applications of Eq. (3.14). A typical SC cross section is a smooth curve (see Papers I-IV) and, thus, the integral in Eq. (3.14) can be easily evaluated using standard numerical techniques. However, quantum mechanical (PT and OP) cross sections usually have a complex resonance structure and the widths of some of those resonances can be vanishingly small (see e.g. Refs. [9, 13–16, 24, 25] and Papers I-IV). Such features make it practically impossible to evaluate the integral in Eq. (3.14) numerically. Moreover, the PT approach tends to overestimate the heights for the long-lived resonances with the tunneling width being smaller than or comparable to the radiative width [9, 14]. Thus, using the PT cross section in Eq. (3.14) for the calculation of the rate coefficient is not correct in the first place. It is obvious, that some other approach is required.

The established method to account for the resonance contribution to the radiative association rate constant is the Breit–Wigner theory [33, 34]. First, the rate constant is divided into two terms

$$k_{\Lambda S\to\Lambda' S}(T) = k^{\mathrm{dir}}_{\Lambda S\to\Lambda' S}(T) + k^{\mathrm{res}}_{\Lambda S\to\Lambda' S}(T), \quad (3.15)$$

where $k^{\mathrm{dir}}_{\Lambda S\to\Lambda' S}(T)$ is the direct contribution, which arises from the baseline of the cross section, and $k^{\mathrm{res}}_{\Lambda S\to\Lambda' S}(T)$ is the contribution due to quantum mechanical resonances. According to the Breit–Wigner theory the latter is calculated as

$$k^{\mathrm{res}}_{\Lambda S\to\Lambda' S}(T) = \hbar^2 P_{\Lambda S}\left(\frac{2\pi}{\mu k_\mathrm{B}T}\right)^{3/2}\sum_{vJ}\frac{(2J+1)e^{-E_{\Lambda SvJ}/k_\mathrm{B}T}}{1/\Gamma^{\mathrm{tun}}_{\Lambda SvJ} + 1/\Gamma^{\mathrm{rad}}_{\Lambda SvJ\Lambda' S}}, \quad (3.16)$$

where the summation is carried out over all resonances. Here $E_{\Lambda S v J}$ is the energy at the peak of the resonance, $\Gamma^{\mathrm{tun}}_{\Lambda S v J}$ is the tunneling width and $\Gamma^{\mathrm{rad}}_{\Lambda S v J \Lambda' S}$ is the width due to the radiative decay to all final bound levels:

$$\Gamma^{\mathrm{rad}}_{\Lambda S v J \Lambda' S} = \hbar \sum_{v' J'} A_{v J v' J'}. \tag{3.17}$$

Here $A_{v J v' J'}$ is the Einstein A coefficient for spontaneous emission from the initial quasi-bound state (v, J) to the final bound state $(v' J')$.

Chapter 4

Quantum dynamical methods

Devil is in the detail.

The present chapter provides a brief summary of the quantum dynamical methods used in this thesis. In quantum mechanics solution of any dynamical problem can be obtained within the time-dependent or time-independent formalism and the choice depends on the problem at hand. In the case of radiative association the low temperature rate constants and, consequently, the low-energy part of the cross sections are usually desired. This makes application of time-dependent methods numerically complicated since very long propagation times and very wide initial wave packets are required [10]. Thus, the time-independent approach has been chosen for the simulation of the radiative association process.

4.1 Bound states

Various methods developed for the calculations of the bound states can be grouped into two general categories: methods using a basis or grid representation of the problem and methods based on the numerical integration of the Schrödinger equation. In this section two methods used in the theses to obtain bound state energies and wavefunctions are described.

4.1.1 Discrete Variable Representation

One of the most common techniques to find eigenvalues and eigenfunctions of the Hamiltonian operator corresponding to the bound states is the discrete variable representation (DVR) method. The general theory of the

method is well described in the literature (e.g see [35, 36]). Here a brief summary of the main ideas is presented.

Without a loss of generality let us consider a one-dimensional time-independent Schrödinger equation (TISE)

$$\hat{H}(x)\Psi(x) = E\Psi(x) \tag{4.1}$$

with a Hamiltonian operator

$$\hat{H}(x) = \hat{T}(x) + V(x) = -\frac{\hbar^2}{2m}\frac{d^2}{dx^2} + V(x). \tag{4.2}$$

The eigenfunction $\Psi(x)$ is expanded in an orthonormal complete basis $\{\phi_n\}$:

$$\Psi(x) = \sum_n a_n(x)\phi_n(x), \tag{4.3}$$

and the expansion coefficients $a_n(x)$ are given by the integral

$$a_n(x) = \int_{-\infty}^{\infty} \phi_n^*(x)\Psi(x)dx. \tag{4.4}$$

If a truncated basis set consisting of N functions $\{\phi_n(x), n = 1, ..., N\}$ is used then we define the variational basis representation (VBR) of an operator in such a basis as

$$\mathbb{A}_{ij}^{\mathrm{VBR}} = \langle\phi_i|\hat{A}|\phi_j\rangle = \int_{-\infty}^{\infty} \phi_i^*(x)\hat{A}\phi_j(x)dx. \tag{4.5}$$

The name applies since, according to the variational principle, the eigenvalues obtained using an N-function representation of the Hamiltonian operator (4.2) are higher than or equal to those of the original problem.

Using the spatial grid $\{x_k\}$ of N points the integrals (4.4) and (4.5) can be approximated by the corresponding numerical quadratures as

$$a_n(x) \approx \sum_{k=1}^{N} \omega_k^{1/2}\phi_n^*(x_k)\Psi(x_k), \tag{4.6}$$

$$\mathbb{A}_{ij}^{\mathrm{VBR}} \approx \sum_{k=1}^{N} \omega_k\phi_i^*(x_k)\left(\hat{A}\phi_j\right)(x_k), \tag{4.7}$$

where ω_k is the quadrature weight. It was shown [36] that there exists a general unitary transformation between the N-dimensional functional space (VBR) and the N-dimensional point space (DVR) representations. Thus, if a

VBR matrix of an operator is known then the discrete variable representation matrix can be calculated as

$$\mathbb{A}^{\mathrm{DVR}} = \mathbb{U}\mathbb{A}^{\mathrm{VBR}}\mathbb{U}^{\dagger}. \tag{4.8}$$

The transformation matrix is given by

$$\mathbb{U} = \mathbb{M}^{-\frac{1}{2}}\mathbb{Y}^{\dagger}, \tag{4.9}$$

where $\mathbb{Y}^{\dagger}_{i,j} = \phi^{\star}_i(x_j)$ and $\mathbb{M} = \mathbb{Y}^{\dagger}\mathbb{Y}$. Constructed in such a way DVR is isomorphic with VBR and can be used, for example, to recover the coordinate dependence of a function from its matrix elements.

In most practical applications coordinate operators are (usually) approximated in the DVR by their values at the grid points. This approximation greatly simplifies construction of the DVR matrix of the potential $V(x)$, since it becomes diagonal:

$$\mathbb{V}^{\mathrm{DVR}}_{ij} = V(x_i)\delta_{ij}. \tag{4.10}$$

However, it has strong consequences making DVR a non-variational method [36], which means that the computed energies of states can be higher or lower than the true eigenenergies. Nevertheless, in general it is possible to converge the results by increasing the number of grid points involved in the calculation.

Choosing spatial grid $\{x_i\}$ judiciously one could construct a DVR matrix for the kinetic energy, which is the most suitable for the problem at hand. One of the most universal and most common choice is a uniform grid, suggested by Colbert and Miller [37]. Consider a one-dimensional system with the Hamiltonian (4.2), where the coordinate x is restricted to the interval (a, b). The grid points are defined as

$$x_i = a + \frac{(b-a)}{N}i, \tag{4.11}$$

and the associated basis functions are given by

$$\phi_n(x) = \frac{2}{b-a}\sin\left(\frac{n\pi(x-a)}{(b-a)}\right). \tag{4.12}$$

Since $\phi_n(x_0 = a) = \phi_n(x_N = b) = 0$ there are a total number of $N-1$ basis functions and corresponding points.

The matrix elements of the kinetic energy operator in the DVR are defined as

$$\mathbb{T}^{\mathrm{DVR}}_{ij} = -\frac{\hbar^2}{2m}\Delta x\sum_{n=1}^{N-1}\phi_n(x_i)\frac{d^2\phi_n(x_j)}{dx^2}, \tag{4.13}$$

where $\Delta x = \frac{b-a}{N}$ is the grid spacing. Calculating the second derivative in Eq. (4.13) and substituting the expressions for x_i the general formula for the kinetic energy matrix elements in the DVR is obtained

$$\mathbb{T}_{ij}^{\mathrm{DVR}} = \frac{\hbar^2}{mN}\left(\frac{\pi}{b-a}\right)^2 \sum_{n=1}^{N-1} n^2 \sin\left(\frac{n\pi i}{b-a}\right)\sin\left(\frac{n\pi j}{b-a}\right). \tag{4.14}$$

Since in the present study DVR is applied to a radial coordinate R, which changes in the interval $(0,\infty)$, a simplified formula for the matrix elements can be obtained [37]:

$$\mathbb{T}_{ij}^{\mathrm{DVR}} = -\frac{\hbar^2}{2m\Delta R^2}(-1)^{i-j}\begin{cases} \dfrac{\pi^2}{3} - \dfrac{1}{2i^2} & i = j \\ \dfrac{2}{(i-j)^2} - \dfrac{2}{(i+j)^2} & i \neq j \end{cases} \tag{4.15}$$

4.1.2 Renormalized Numerov method

Another family of methods is based on the use of numerical integration techniques to calculate bound state wavefunctions.[1] Here we are going to describe a method, originally proposed by Johnson [38, 39], which is using the renormalized Numerov algorithm for integration of differential equations.

Solution of many multidimensional quantum mechanical problems is based on the expansion of the total wavefunction in a basis set of the following type

$$\Psi(R,q) = \sum_{n=1}^{N} \frac{1}{R}\psi_n(R)\phi_n(q), \tag{4.16}$$

where R is the radial coordinate, which usually changes the most for the problem at hand, $\psi_n(R)$ are the radial wavefunctions and $\phi_n(q)$ are some appropriate orthonormal basis functions, which depend on all other coordinates of the system. Substitution of the expansion (4.16) into the Schrödinger equation transforms the original problem of solving a partial differential equation for the total wavefunction $\Psi(R,q)$ into the problem of solving a system of N coupled ordinary differential equations for $\psi_n(R)$. The latter is also known in literature as the coupled-channel Schrödinger equation and can be written as

$$\left[\mathbb{I}\frac{d^2}{dR^2} + \mathbb{Q}(R)\right]\psi(R) = 0, \tag{4.17}$$

[1] Also known in literature as propagation or "shooting" methods.

where $\mathbb{I}$ is the unit matrix, $\psi(R)$ is the N-component vector wavefunction with elements $\psi_n(R)$ and

$$\mathbb{Q}(R) = \frac{2\mu}{\hbar^2}\left[E\mathbb{I} - \mathbb{V}(R)\right]. \tag{4.18}$$

Here μ is the reduced mass of the system, E is the energy of the bound state and $\mathbb{V}(R)$ is the potential energy matrix in the basis $\{\phi_n(q)\}$. All terms corresponding to the rotational kinetic energy are assumed to be included in $\mathbb{V}(R)$.

Numerical solution of Eq. (4.17) requires the knowledge of the wavefunction's derivative at the boundaries. In order to avoid this, N linearly independent solutions with linearly independent derivatives can be calculated simultaneously [40]. Those solutions are grouped into a $N \times N$ matrix $\Psi(R)$, which replaces $\psi(R)$ in eq. (4.17):

$$\left[\mathbb{I}\frac{d^2}{dR^2} + \mathbb{Q}(R)\right]\Psi(R) = 0. \tag{4.19}$$

The columns of $\Psi(R)$ span the whole space of initial derivatives and, thus, the correct vector wavefunction $\psi(R)$ is defined by some linear combination of those.

Numerical solution of Eq. (4.19) can be obtained using the Numerov method, which requires the equally spaced grid $\{R_k, k = 0, ..., K\}$ to be chosen. When the grid is set, the wavefunction matrix $\Psi(R)$ can be calculated using the three-points recursion relation:

$$[\mathbb{I} - \mathbb{T}_{k+1}]\Psi_{k+1} - [2\mathbb{I} + 10\mathbb{T}_k]\Psi_k + [\mathbb{I} - \mathbb{T}_{k-1}]\Psi_{k-1} = 0, \tag{4.20}$$

where $\Psi_k = \Psi(R_k)$, and

$$\mathbb{T}_k = -\frac{\Delta R^2}{12}\mathbb{Q}(R_k) \tag{4.21}$$

with ΔR being the grid spacing and the index k runs from 0 to K. Let us define the following matrices

$$\mathbb{W}_k = \mathbb{I} - \mathbb{T}_k, \tag{4.22}$$

$$\mathbb{F}_k = \mathbb{W}_k\Psi_k. \tag{4.23}$$

Substitution of $\mathbb{F}_k$ into Eq. (4.20) gives

$$\mathbb{F}_{k+1} - \mathbb{U}_k\mathbb{F}_k + \mathbb{F}_{k-1} = 0, \tag{4.24}$$

where $\mathbb{U}_k = 12\mathbb{W}_k^{-1} - 10\mathbb{I}$. Now defining the ratio matrix as

$$\mathbb{R}_k = \mathbb{F}_{k+1}\mathbb{F}_k^{-1} \tag{4.25}$$

and substituting it into Eq. (4.24) we arrive at the two-point renormalized Numerov recurrence

$$\mathbb{R}_k = \mathbb{U}_k - \mathbb{R}_{k-1}^{-1}. \tag{4.26}$$

The inward solution of Eq. (4.19), when the integration starts at the outer boundary R_K and continues to R_0, can be obtained using a similar relation

$$\hat{\mathbb{R}}_k = \mathbb{U}_k - \hat{\mathbb{R}}_{k+1}^{-1}, \tag{4.27}$$

where

$$\hat{\mathbb{R}}_k = \mathbb{F}_{k-1}\mathbb{F}_k^{-1}. \tag{4.28}$$

The initial conditions for Eqs. (4.26) and (4.27) are given by

$$\mathbb{R}_0 = \hat{\mathbb{R}}_K = 0. \tag{4.29}$$

Those can be used for all cases, except when the second derivative of the wavefunction is not equal to zero at the boundaries. A detailed discussion of that issue and possible solutions can be found in Ref. [39].

From Eq. (4.19) the bound state energies can be obtained by an iterative procedure, which is based on counting nodes of the wavefunction. If eigenvalues are sorted in ascending order, and each of them is labeled by a vibrational quantum number v then, according to the oscillation theorem, the corresponding wavefunction has v nodes. Johnson [39] defined the node of a multichannel wavefunction as a point at which $\det|\Psi(R)| = 0$. Thus, if there is a node between two adjacent grid points then in terms of the $\mathbb{R}$ matrices used in the renormalized Numerov method the corresponding condition reads $\det|\mathbb{R}_k| < 0$. In order to avoid miscounting when there is more than one node per grid step, the ratio matrix (4.25) is diagonalized at every grid point and the number of its negative elements is tracked.

The procedure of finding the energy of the n-th bound state includes the following steps:

1. Define the energy interval (E_l, E_h), which contains the desired eigenvalue.[2]

2. Using Eq. (4.26), construct the outward solution at the trial energy $E = (E_h + E_l)/2$ and count the nodes of the wavefunction.

3. If the node count is greater than n, then set $E_h = E$ else set $E_l = E$.

4. Repeat steps 2 and 3 until the desired convergence is reached.

[2]The obvious interval, which contains energies of all bound states of the system is from the bottom of the potential to the dissociation limit.

The procedure above is general and will converge to correct energies even when the system has degenerate bound states.

In order to calculate the wavefunction, the inward and outward solutions of Eq. (4.19) are constructed first. The proper bound state wavefunction and its first derivative must be continuous. The alternative requirement is that the inward and outward solutions are equal at two adjacent grid points,

$$\Psi_o(R_m) \cdot \mathbf{o} = \Psi_i(R_m) \cdot \mathbf{i} = \psi(R_m), \tag{4.30}$$

$$\Psi_o(R_{m+1}) \cdot \mathbf{o} = \Psi_i(R_{m+1}) \cdot \mathbf{i} = \psi(R_{m+1}), \tag{4.31}$$

where subscripts o/i mark the outward and inward solutions and $\mathbf{o}$ and $\mathbf{i}$ are some unknown vectors. Using Eqs. (4.22)-(4.23) the same conditions can be written as

$$\mathbb{F}_o(R_m) \cdot \mathbf{o} = \mathbb{F}_i(R_m) \cdot \mathbf{i} = \mathbf{f}(R_m), \tag{4.32}$$

$$\mathbb{F}_o(R_{m+1}) \cdot \mathbf{o} = \mathbb{F}_i(R_{m+1}) \cdot \mathbf{i} = \mathbf{f}(R_{m+1}), \tag{4.33}$$

where

$$\mathbf{f}(R_m) = [\mathbb{I} - \mathbb{T}_m]\psi(R_m). \tag{4.34}$$

Substituting the definitions of the ratio matrices (4.25) and (4.28) into Eq. (4.33) gives

$$\mathbb{R}_m \mathbb{F}_o(R_m) \cdot \mathbf{o} = \hat{\mathbb{R}}_{m+1}^{-1} \mathbb{F}_i(R_m) \cdot \mathbf{i}. \tag{4.35}$$

Finally, combining Eqs. (4.32) and (4.35) we obtain the following equation for the vector $\mathbf{f}(R_m)$

$$[\mathbb{R}_m - \hat{\mathbb{R}}_{m+1}^{-1}]\mathbf{f}(R_m) = 0. \tag{4.36}$$

The above equation is the eigenvector problem. The eigenvalues of the matrix $\mathbb{R}_m - \hat{\mathbb{R}}_{m+1}^{-1}$ are calculated at every point and the matching point R_m is chosen as the one at which the eigenvalue closest to zero is found. When $\mathbf{f}(R_m)$ is known the vectors $\mathbf{f}(R_k)$ are obtained as

$$\mathbf{f}(R_k) = \mathbb{R}_k^{-1}\mathbf{f}(R_{k+1}),\ k = m-1, m-2, ..., 0 \tag{4.37}$$

$$\mathbf{f}(R_k) = \hat{\mathbb{R}}_k^{-1}\mathbf{f}(R_{k-1}),\ k = m+1, m+2, ..., K \tag{4.38}$$

and the corresponding bound state wavefunction $\psi(R_k)$ is calculated using Eq. (4.34).

The main advantage of the described renormalized Numerov method is that the eigenenergies can be calculated with an arbitrary precision, which is set in advance. This is especially useful when the system has bound states very close to (within 1 cm^{-1}) the dissociation limit. Also, the method naturally allows calculation of a subset of states within a certain energy range. As drawbacks we should mention that it gives only one state at a time and relatively dense spatial grids are required to perform accurate calculations.

4.2 Continuum states

In the present thesis the calculation of the continuum wavefunctions was done only for the single-channel problems, and the method is described below.

We are looking for solutions of the time-independent Schrödinger equation

$$\hat{\mathrm{H}}\Psi = E\Psi, \tag{4.39}$$

which correspond to positive energies [3]. The Hamiltonian operator in spherical polar coordinates is given by

$$\hat{\mathrm{H}} = -\frac{\hbar^2}{2\mu R}\frac{\partial^2}{\partial R^2}R + \frac{\hat{\ell}^2}{2\mu R^2} + V(R). \tag{4.40}$$

Here $V(R)$ is the potential energy function and $\hat{\ell}$ is the orbital angular momentum operator:

$$\hat{\ell}^2 = -\hbar^2\left[\frac{1}{\sin\theta}\frac{\partial}{\partial\theta}\left(\sin\theta\frac{\partial}{\partial\theta}\right) + \frac{1}{\sin^2\theta}\frac{\partial^2}{\partial\phi^2}\right]. \tag{4.41}$$

It is a well-known [23] that the eigenfunctions of the Hamiltonian (4.40) can be expressed as a product of the radial and angular parts:

$$\Psi_{Elm}(R,\theta,\phi) = \psi_{E\ell}(R)\mathrm{Y}_{\ell m}(\theta,\phi), \tag{4.42}$$

where $\mathrm{Y}_{\ell m}(\theta,\phi)$ are the spherical harmonics [41]. Substitution of (4.42) into (4.39) gives the radial equation for $\psi_{E\ell}(R)$. Asymptotically, when the potential $V(R)$ is negligible, it reduces to the free-particle Schrödinger equation:

$$\left(\frac{d^2}{dR^2} + \frac{2}{R}\frac{d}{dR} - \frac{\ell(\ell+1)}{R^2} + k^2\right)\psi_{E\ell}(R) = 0, \tag{4.43}$$

where $k = \frac{\sqrt{2\mu E}}{\hbar}$. Using the substitution $\rho = kR$, Eq. (4.43) can be rewritten as

$$\left(\frac{d^2}{d\rho^2} + \frac{2}{\rho}\frac{d}{d\rho} + 1 - \frac{\ell(\ell+1)}{\rho^2}\right)\psi_{E\ell}(\rho) = 0. \tag{4.44}$$

The last equation is the spherical Bessel equation, particular solutions of which are known to be the spherical Bessel and the spherical Neumann functions:

$$j_\ell(\rho) = \left(\frac{\pi}{2\rho}\right)^{\frac{1}{2}} J_{\ell+\frac{1}{2}}(\rho) \tag{4.45}$$

$$n_\ell(\rho) = (-1)^{\ell+1}\left(\frac{\pi}{2\rho}\right)^{\frac{1}{2}} J_{-\ell-\frac{1}{2}}(\rho) \tag{4.46}$$

[3] It is assumed that the energy is set to be zero at the dissociation limit.

and $J_\nu(\rho)$ is the ordinary Bessel function of the order ν [42]. Thus, the radial wavefunction is given by the linear combination:

$$\psi_{E\ell}(R) = B_\ell j_\ell(kR) + C_\ell n_\ell(kR). \tag{4.47}$$

The coefficients B_ℓ and C_ℓ can be complex, but their ratio must be real for hermitian Hamiltonians. Using the asymptotic expressions for $j_\ell(kR)$ and $n_\ell(kR)$ we can write

$$\psi_{E\ell}(R) \overset{R\to\infty}{\to} \frac{1}{kR}\left[B_\ell \sin\left(kR - \frac{\ell\pi}{2}\right) - C_\ell \cos\left(kR - \frac{\ell\pi}{2}\right)\right], \tag{4.48}$$

Introducing the quantities A_ℓ and δ_ℓ, such that

$$B_\ell = A_\ell \cos\delta_\ell, \tag{4.49}$$
$$C_\ell = -A_\ell \sin\delta_\ell, \tag{4.50}$$

Eq. (4.48) reduces to

$$\psi_{E\ell}(R) \overset{R\to\infty}{\to} \frac{A_\ell}{kR}\sin\left(kR - \frac{\ell\pi}{2} + \delta_\ell\right), \tag{4.51}$$

where

$$\delta_\ell = \arctan\left(-\frac{C_\ell}{B_\ell}\right). \tag{4.52}$$

The quantity δ_ℓ is called the phase shift and characterize the strength of the scattering.

The radial part of the continuum wave function can be calculated by numerical integration of Eq. (4.43) using the Numerov method [43]. However, to get the correct normalization, knowledge of the phase shift is required. The numerical calculation of the phase shift is done in a few steps. First, Eq. (4.43) is numerically integrated to the point R_0, at which the wavefunction is assumed to have asymptotic behavior. [4] Then, the integration is continued to the point R_i, where the wavefunction equals zero. At this point the trial phase shift is calculated using Eqs. (4.47) and (4.52)

$$\delta_i = \arctan\left(\frac{j_\ell(kR_i)}{n_\ell(kR_i)}\right). \tag{4.53}$$

Then, Eq. (4.43) is integrated to the next point, at which the wavefunction vanishes R_{i+1}, and the new phase shift δ_{i+1} is calculated in the same way.

[4] The location of such a point strongly depends on the form of the potential and should be found for the particular calculation.

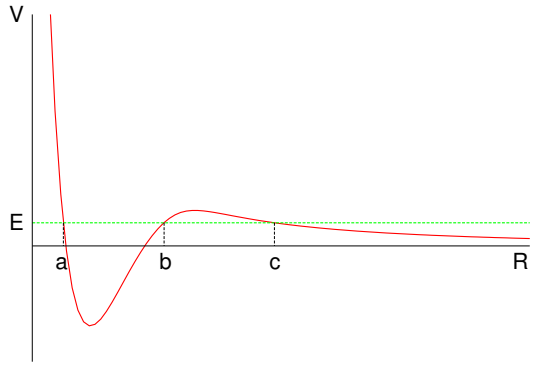

Figure 4.1: Schematic effective potential energy diagram. For a collision energy E the classical turning points are shown by small letters.

The procedure is repeated until the set of phase shifts $\{\delta_i\}$ converges to the final value. Finally, the integrated wavefunction is normalized according to

$$\psi_{E\ell}(R_0) * N = j_\ell(kR_0)\cos\delta - n_\ell(kR_0)\sin\delta, \tag{4.54}$$

where N is the normalization constant.

4.3 Quasi-bound states

In order to apply the Breit–Wigner analysis to compute the resonance contribution to the radiative association rate coefficient (3.16) the parameters of quasi-bound states (which manifest themselves in the cross section as resonances) should be known. In the present thesis such parameters are calculated using Le Roy's LEVEL program [44], in which the Airy function boundary conditions are implemented to obtain the quasi-bound state wavefunctions. A short summary of the method is given below and for additional details and explanations the reader is referred to Ref. [45].

In this section we will consider the effective potential with a centrifugal barrier, which has three classical turning points (see Fig. 4.1). The radial wavefunction $\psi_{E\ell}(R)$ of a quasi-bound state with the energy E and the orbital angular momentum quantum number ℓ obeys the equation

$$\left(\frac{d^2}{dR^2} + k^2 - V_\ell(R)\right)\psi_{E\ell}(R) = 0, \tag{4.55}$$

where k is defined in section 4.2 and the effective potential is given by

$$V_\ell(R) = \frac{2\mu V(R)}{\hbar^2} + \frac{\ell(\ell+1)}{R^2}. \tag{4.56}$$

Using the semi-classical approximation the wavefunction $\psi_{E\ell}(R)$ in the asymptotic region ($R \gg c$) can be written as [45]

$$\psi_{E\ell}(R) \sim \frac{1}{\sqrt{k_\ell(R)}} \left(C' \exp\left[i \int_c^R k_\ell(R) dR \right] + C'' \exp\left[-i \int_c^R k_\ell(R) dR \right] \right), \tag{4.57}$$

where $k_\ell(R) = \sqrt{k^2 - V_\ell(R)}$. The coefficients C' and C'' satisfy the equations:

$$\begin{pmatrix} C' \\ C'' \end{pmatrix} = \frac{1}{2}\sqrt{\frac{2\mu}{\pi\hbar^2 k}} \begin{pmatrix} e^{i\delta} \\ e^{-i\delta} \end{pmatrix} \tag{4.58}$$

with the semi-classical phase shift δ given by

$$\delta = \arctan(e^{-2\gamma} \tan\alpha_\ell) + \frac{\theta - \phi}{2} - \frac{\pi}{4}, \tag{4.59}$$

$$\alpha_\ell = \int_a^b k_\ell(R) dR - \frac{\theta + \phi}{2}. \tag{4.60}$$

Here γ, θ, ϕ are phase integrals over different parts of the effective potential.

The main difference between quasi-bound and truly continuum states is in the amplitude of the wavefunction in the region between a and b turning points. It was shown [45] that this amplitude reaches its maximum when

$$\alpha_\ell = \pi \left(v + \frac{1}{2} \right). \tag{4.61}$$

Thus, Eq. (4.61) is the semi-classical quantization conditions, where v is the vibrational quantum number assigned to the quasi-bound level. In order to use this equation one needs to know values of the phase integrals γ, θ, ϕ. One way to determine them is to use the Airy functions boundary conditions.

For an energy E well below the top of the centrifugal barrier, where the turning points a, b and c are well separated, at the outermost turning point $V_\ell(R)$ can be approximated by a straight line

$$V_\ell(R) = k^2 - (R - c)\frac{dV_\ell(R_c)}{dR}. \tag{4.62}$$

Then the asymptotic form of the radial wavefunction $\psi_{E\ell}(R)$ can be expressed in terms of Airy functions as

$$\psi_{E\ell}(R) \sim \left(\frac{z}{k_\ell^2(R)}\right)^{\frac{1}{4}} \Big(D_1 \mathrm{Ai}(-z) + D_2 \mathrm{Bi}(-z)\Big), \tag{4.63}$$

where $\mathrm{Ai}(-z)$, $\mathrm{Bi}(-z)$ are the Airy functions of the first and second kind, D_1 and D_2 are distance independent coefficients [45] and

$$z = (R - c)\left[\frac{dV_\ell(R_c)}{dR}\right]^{\frac{1}{3}}. \tag{4.64}$$

Using the same linear approximation for $V_\ell(R)$ at the second turning point allows for construction of a similar form of the radial wavefunction in the region (a, b). Matching it to $\psi_{E\ell}(R)$ given by Eq. (4.63) gives semi-classical expressions for the phase integrals:

$$\gamma = \int_b^c |k_\ell(R)| + \ln 2, \tag{4.65}$$

$$\theta = \phi = 0. \tag{4.66}$$

Together Eqs. (4.60), (4.61) and (4.66) allow us to determine the energies $E_{\ell v}$ of the quasi-bound levels.

When the energies are known the tunneling widths ($\Gamma_{\ell v}^{\mathrm{tun}}$) are calculated as [46]

$$\Gamma_{\ell v}^{\mathrm{tun}} = 2\omega[\epsilon_\ell(E_{\ell v})] \left(\frac{d\alpha_\ell(E_{\ell v})}{dE}\right)^{-1}, \tag{4.67}$$

where the explicit form of the function $\omega[\epsilon_\ell(E)]$ is defined in Eq. (3.7) in Ref. [46]. The radiative widths $\Gamma_{\ell v}^{\mathrm{rad}}$ are obtained using Eq. (3.17), where the Einstein coefficient $A_{\ell v \ell' v'}$ is calculated from the transition dipole moment $D(R)$, the corresponding bound state wavefunction $\psi_{\ell' v'}$ and the quasi-bound state wavefunction in the region (a, b).

The method gives highly accurate results for the parameters of the low-lying quasi-bound levels and for the levels close to the top of the centrifugal barrier the inaccuracy in width is estimated to be 10-20% [45]. Unfortunately, the method does not work for broad resonances just above the centrifugal barrier.

4.4 L^2-type methods for the calculation of cross sections

A typical calculation of the radiative association cross section within the perturbation theory formalism requires the computation of the bound and

scattering wavefunctions (corresponding numerical methods are described in Sec. 4.1 and 4.2) and the matrix elements of the dipole moment operator between them. An alternative approach which eliminates the necessity of solving the scattering problem relies on non-hermitian quantum mechanics. In such an approach the Hamiltonian operator is modified by the addition of a complex absorbing potential (CAP) or by the complex scaling (CS) of the reaction coordinate and an L^2 method (such as DVR) is used to obtain a discrete set of eigenstates with complex eigenvalues:

$$\left(\tilde{\Psi}_u, E_u - \frac{i}{2}\Gamma_u\right).$$

Those eigenstates can be used instead of the continuum states in calculations of the dipole operator matrix elements in Eq. (3.1).

L^2-type methods were successfully applied for calculations of the positions and widths of resonances [47], to model photodissociation [48, 49] and radiative association [26] processes. In Paper V the CAP method was applied to study the role of non-adiabatic couplings in radiative association of $C(^3P)$ and $N(^4S)$ atoms and here a brief summary is presented.

The square of the dipole operator matrix element in Eq. (3.1) can be written as [48]

$$|\langle\Psi_{nJME}|\hat{\mathrm{D}}|\Psi_{J'M'v'}\rangle|^2 = |\langle\Phi_{nJME}|\epsilon\hat{\mathrm{G}}^+(E_t)\hat{\mathrm{D}}|\Psi_{J'M'v'}\rangle|^2, \tag{4.68}$$

where $E_t = E + V_n(\infty)$ is the total energy of the system, Φ_{nJME} is defined by the asymptotic boundary conditions and

$$\hat{\mathrm{G}}^+(E_t) = \lim_{\epsilon\to\infty} \frac{1}{E_t + i\epsilon - \hat{\mathrm{H}}} \tag{4.69}$$

is the Green operator. The key idea of the CAP method is to use the modified Green operator in Eq. (4.68)

$$\tilde{\mathrm{G}}^+(E_t) = \frac{1}{E_t - \tilde{\mathrm{H}}}, \tag{4.70}$$

where $\tilde{\mathrm{H}}$ is obtained from the Hamiltonian operator by adding a complex absorbing potential:

$$\tilde{\mathrm{H}} = \hat{\mathrm{H}} - iW, \tag{4.71}$$

where W is a real positive function of R. Thus, Eq. (4.68) transforms to

$$|\langle\Psi_{nJME}|\hat{\mathrm{D}}|\Psi_{J'M'v'}\rangle|^2 = |\langle\Phi_{nJME}|W\tilde{\mathrm{G}}^+(E_t)\hat{\mathrm{D}}|\Psi_{J'M'v'}\rangle|^2. \tag{4.72}$$

As noted in the Ref. [48] adding a CAP to the Hamiltonian operator is equivalent to interpreting the formal convergence parameter ϵ in Eq. (4.69) as a coordinate dependent operator.

The spectral resolution of the Green operator (4.70) can be expressed in terms of the eigenfunctions of the modified Hamiltonian $\tilde{\mathrm{H}}$:

$$\tilde{\mathrm{G}}^{+}(E_t) = \sum_u \frac{|\tilde{\Psi}_{JMu})(\tilde{\Psi}_{JMu}|}{E_t - E_{Ju} + \frac{i}{2}\Gamma_{Ju}}. \tag{4.73}$$

It should be noted that the proper normalization of $\tilde{\Psi}_{JMu}$ requires the use of the so-called C-product [47]:

$$(\tilde{\Psi}_{JMu}|\tilde{\Psi}_{JMu'}) = \langle\tilde{\Psi}^{*}_{JMu}|\tilde{\Psi}_{JMu'}\rangle = \int_V \Psi_{JMu}\Psi_{JMu'}dV = \delta_{uu'}. \tag{4.74}$$

Substitution of Eq. (4.73) into Eq. (4.72) gives the working formula for the matrix elements of the dipole operator

$$|\langle\Psi_{nJME}|\hat{\mathrm{D}}|\Psi_{J'M'v'}\rangle|^2 = \left|\sum_u \frac{(\Phi_{nJME}|W|\tilde{\Psi}_{JMu})(\tilde{\Psi}_{JMu}|\hat{\mathrm{D}}|\Psi_{J'M'v'})}{E_t - E_{Ju} + \frac{i}{2}\Gamma_{Ju}}\right|^2 \tag{4.75}$$

If all initial channels of the system are asymptotically degenerate and we choose $V_n\infty = 0$, i.e. $E_t = E$, then Eq. (4.75) can be simplified to the following form [26, 48]

$$|\langle\Psi_{nJME}|\hat{\mathrm{D}}|\Psi_{J'M'v'}\rangle|^2 = -\frac{1}{\pi}\mathrm{Im}\sum_u \frac{(\tilde{\Psi}_{JMu}|\hat{\mathrm{D}}|\Psi_{J'M'v'})^2}{E - E_{Ju} + \frac{i}{2}\Gamma_{Ju}}. \tag{4.76}$$

In the presented approach the complex absorbing potential (CAP) is basically a mathematical tool, which is used to modify the asymptotic behavior of the wavefunctions corresponding to the continuum spectrum. The only requirement imposed on the CAP is that it does not perturb the dynamics of the system in the interaction region and its actual functional form is, otherwise, arbitrary. In contrast, in the optical potential (OP) method described in Sec. 3.1.2 the imaginary potential is meant to alter the dynamics of the system and penetrates the interaction region. However, the form of OP is chosen in a specific way which mimics the radiative decay by spontaneous emission.

Chapter 5

Summary of included papers

The research presented in this thesis is based on Papers I-V, which are included in the printed version. Due to this fact, in the current chapter merely an abstract and highlights of the obtained results are given. For full details the reader is referred to the corresponding papers at the end of this thesis.

5.1 Diatomic systems

In Papers I-IV the formation of the CN, SiN, SiP and CO molecules through radiative association of the corresponding atoms in their ground electronic states is studied by the methods described in Chapter 3. In all cases the Born-Oppenheimer approximation is employed. The considered molecules possess a certain astrochemical interest and their formation rates are of importance [4, 50–54] and, thus, the emphasis is on the calculation of the rate coefficients.

Paper I

In Paper I the formation of the CN radical in the two lowest electronic states $X^2\Sigma^+$ and $A^2\Pi$ through radiative association of C(^3P) and N(^4S) atoms is investigated using the PT and SC approaches. This process can occur through four reactions:

$$\mathrm{C}(^3P) + \mathrm{N}(^4S) \rightarrow \mathrm{CN}(A^2\Pi) \rightarrow \mathrm{CN}(X^2\Sigma^+) + h\nu, \tag{5.1}$$

$$\mathrm{C}(^3P) + \mathrm{N}(^4S) \rightarrow \mathrm{CN}(A^2\Pi) \rightarrow \mathrm{CN}(A^2\Pi) + h\nu, \tag{5.2}$$

$$\mathrm{C}(^3P) + \mathrm{N}(^4S) \rightarrow \mathrm{CN}(X^2\Sigma^+) \rightarrow \mathrm{CN}(X^2\Sigma^+) + h\nu, \tag{5.3}$$

$$\mathrm{C}(^3P) + \mathrm{N}(^4S) \rightarrow \mathrm{CN}(X^2\Sigma^+) \rightarrow \mathrm{CN}(A^2\Pi) + h\nu. \tag{5.4}$$

The cross sections for reaction (5.1) are calculated using the PT and SC approaches and the radiative association rate coefficient is presented for $T = 40 - 2\ 000$ K. Comparison shows (Fig. 1 in Paper I) that the SC cross section fits the baseline of the PT one well and, thus, the former can be used to determine the direct component of the rate coefficient. The obtained direct contribution (Table I in Paper I) is in good agreement with the results of the SC study published previously by Singh and Andreazza [8]. The resonance contribution was found to be significant for $T < 2\ 000$ K. At room temperature it amounts to 25% of the total rate constant. The overall effect, however, is much less important than for hydrogen-containing species (see e.g. [7, 9, 13]).

The radiative association through reactions (5.2)-(5.4) is considered and the corresponding PT cross sections are computed. Comparison of all four cross sections establishes that the baseline for the $A^2\Pi \rightarrow X^2\Sigma^+$ transition is several orders of magnitude higher than for the other transitions. Therefore, the contribution to the radiative association rate coefficient from the other transitions is expected to be negligible.

It should be noted that the calculated direct component of the rate constant is based on the unrestricted transition rate (3.6) rather than on the restricted one (3.12). However, since the rate coefficient is not calculated for $T > 2\ 000$ K, it should not affect the results of the study.

Paper II

Paper II is devoted to comparison of various methods for calculations of the radiative association cross sections, which are described in Chapter 3. The advantages and limitations of each approach are presented and those are applied to study the formation of SiN through the following transitions

$$\mathrm{Si}(^3P) + \mathrm{N}(^4S) \rightarrow \mathrm{SiN}(A^2\Pi) \rightarrow \mathrm{SiN}(X^2\Sigma^+) + h\nu, \tag{5.5}$$

$$\mathrm{Si}(^3P) + \mathrm{N}(^4S) \rightarrow \mathrm{SiN}(X^2\Sigma^+) \rightarrow \mathrm{SiN}(A^2\Pi) + h\nu. \tag{5.6}$$

A detailed comparison of peak heights of some long-lived ($\Gamma^{\mathrm{tun}} \ll \Gamma^{\mathrm{rad}}$) resonances (Table III in Paper II) shows that the results of the OP method are in a good agreement with the predictions of the Breit–Wigner theory, while the PT approach overestimates the peak heights by one-two orders of magnitude. In the case of resonances for which the tunneling through centrifugal barrier is the dominant channel of decay, i.e. $\Gamma^{\mathrm{tun}} \gg \Gamma^{\mathrm{rad}}$, all three approaches predict similar resonance heights. Unfortunately, the OP method still cannot be used directly to obtain the radiative association rate coefficient, due to numerical reasons (see discussion in Sec. 3.2).

The rate coefficients for reactions (5.5) and (5.6) are calculated for $T = 10 - 20\,000$ K (Fig. 5 in Paper II). A rapid decrease in the rate constant for formation of ground state SiN is observed above 2 000 K which was not seen previously [55] and which is a consequence of using the restricted transition rate (3.12) in the simulation of radiative association. The $A^2\Pi \rightarrow X^2\Sigma^+$ transition is shown to be the main formation channel with the total rate coefficient being roughly an order of magnitude larger than for $X^2\Sigma^+ \rightarrow A^2\Pi$. The resonance contribution to the rate constant of reaction (5.5) monotonically decreases with temperature; it is 35% at $T = 10$ K and is negligible for $T > 500$ K. For the $X^2\Sigma^+ \rightarrow A^2\Pi$ transition the resonances add up to $15 - 25\%$ to the total rate constant for all considered temperatures.

Paper III

In Paper III formation of the SiP radical through radiative association of Si(^3P) and P(^4S) atoms is investigated. The following four reactions are considered

$$\mathrm{Si}(^3P) + \mathrm{P}(^4S) \rightarrow \mathrm{SiP}(A^2\Sigma^+) \rightarrow \mathrm{SiP}(X^2\Pi) + h\nu, \tag{5.7}$$
$$\mathrm{Si}(^3P) + \mathrm{P}(^4S) \rightarrow \mathrm{SiP}(X^2\Pi) \rightarrow \mathrm{SiP}(A^2\Sigma^+) + h\nu, \tag{5.8}$$
$$\mathrm{Si}(^3P) + \mathrm{P}(^4S) \rightarrow \mathrm{SiP}(a^4\Pi) \rightarrow \mathrm{SiP}(b^4\Sigma^+) + h\nu, \tag{5.9}$$
$$\mathrm{Si}(^3P) + \mathrm{P}(^4S) \rightarrow \mathrm{SiP}(b^4\Sigma^+) \rightarrow \mathrm{SiP}(a^4\Pi) + h\nu. \tag{5.10}$$

The radiative association cross sections for all reactions are calculated using the SC and PT methods. The PT cross sections show the same qualitative behavior: complex resonance structure with baselines showing a monotonic decrease up to certain threshold energies above which the cross sections decay fast. The results of the SC calculations reproduce the quantum mechanical baselines for all studied transitions.

Radiative association rate constants are calculated in a wide temperature range 10−20 000 K. Comparison of the direct rate coefficient for reaction (5.7) with the results of the previous semi-classical study [56] reveals a strong disagreement between the two (Fig. 3 in Paper III). While no explanation is found, the author is confident in the results of Paper III, since the direct contribution is calculated from the SC cross section, which agrees well with the baseline of the PT cross sections. Moreover, reasonable agreement for $T = 300 - 2\,000$ K is found between the SC rate coefficients for the $a^4\Pi \rightarrow b^4\Sigma^+$ transition (Fig. 4 in Paper III). The difference at higher T is due to the use of the restricted transition rate in the calculations.

The $X^2\Pi \rightarrow A^2\Sigma^+$ transition is shown to have the biggest rate coefficient and, thus, to be the main channel for formation of SiP. The corresponding

resonance contribution is as big as the direct one at 10 K and monotonically decreases with increasing temperature. For the $A^2\Sigma^+ \rightarrow X^2\Pi$ transition the resonances add up to $10 - 40\%$ of the total rate constant at all considered temperatures. The radiative association rate coefficients for formation of SiP in the quartet spin states (Fig. 4 in Paper III) show the same features as those for the doublets, while being generally smaller by a factor of 2-3 than those for transitions between the doublet states of the same symmetry.

Paper IV

Formation of carbon monoxide (CO) in its ground electronic state $X^1\Sigma^+$ by radiative association is discussed in Paper IV. Previous theoretical studies [11, 25] showed that the two most important formation channels are

$$\mathrm{C}(^3P) + \mathrm{O}(^3P) \rightarrow \mathrm{CO}(A^1\Pi) \rightarrow \mathrm{CO}(X^1\Sigma^+) + h\nu \tag{5.11}$$

and

$$\mathrm{C}(^3P) + \mathrm{O}(^3P) \rightarrow \mathrm{CO}(X^1\Sigma^+) \rightarrow \mathrm{CO}(X^1\Sigma^+) + h\nu. \tag{5.12}$$

The electronic potential of the $A^1\Pi$ state has a barrier of 636 $\mathrm{cm}^{-1} \approx 79$ meV, which determines the low-energy behavior of the cross sections for reaction (5.11). For the energies below the barrier top the SC cross section is zero, but the PT cross section has a finite magnitude coming from the quantum mechanical tunneling through the barrier (Fig. 2 in Paper IV). The difference between the PT and SC cross sections at high collision energies is attributed to the non-Franck–Condon transitions.

The rate constant for reaction (5.11) is calculated for $T = 10{-}20\,000$ K. It is shown that the rate coefficient is dominated by the resonance contribution at temperatures below 600 K and it amounts to 30% at $T = 1\,000$ K (Fig. 4a in Paper IV). The contribution from the $X^1\Sigma^+ \rightarrow X^1\Sigma^+$ transition is found to vary from small ($T = 10$ K) to negligible ($T > 20$) K.

Based on the obtained results it is obvious that the SC theory does not predict the correct rate constant for the radiative association through the $A^1\Pi \rightarrow X^1\Sigma^+$ transition even at relatively large temperatures. The contribution from the quantum mechanical resonances should be included in order to get correct qualitative behavior of the rate coefficient as a function of temperature.

5.2 Special aspects of the process

In the present section some special aspects of the radiative association process, which are left untouched in the majority of the theoretical studies

performed so far and which caught the attention of the author during his time as a doctoral student, are discussed.

5.2.1 Isotope effect

In the previous section it was discussed that the radiative association rate coefficient for the formation of CO through the $A^1\Pi \rightarrow X^1\Sigma^+$ transition at temperatures below 600 K is dominated by the resonance contribution. Those resonances arise due to the quantum mechanical tunneling through the barrier on the $A^1\Pi$ potential. Tunneling is known to depend strongly with the reduced mass, thus a pronounced isotope effect in the corresponding rate constant could be expected.

In Paper IV the formation of the ^{12}CO and ^{13}CO isotopologues through reactions (5.11) and (5.12) is investigated. Comparison of the cross sections reveals that the main differences are in the resonance structure of the PT cross sections for the $A^1\Pi \rightarrow X^1\Sigma^+$ transition at collision energies smaller than the barrier height (Figs. 2 and 3 in Paper IV). The difference is caused by the change in the reduced mass of the system, which affects the vibrational spacing and, ultimately, the resonance structure.

The observed difference in the cross sections translates to the rate coefficients (Fig. 4 in Paper IV). Thus, it is shown that the presence of a barrier on the potential energy curve of the $A^1\Pi$ electronic state leads to different formation channels for the isotopologues of CO at low temperatures. In the case of ^{12}CO the $A^1\Pi \rightarrow X^1\Sigma^+$ transition is the dominant formation channel for $T = 10 - 20\,000$ K. In contrast, for ^{13}CO at $T < 36$ K the rate coefficient for reaction (5.12) is higher than that for reaction (5.11), which is explained by the difference in the resonance contribution between the isotopologues.

Figure 5.2.1 shows the total (summed over various electronic transitions) radiative association rate coefficients for the formation of the considered isotopologues. As can be seen from the figure for $T < 100$ K the overall rate constant for formation of ^{12}CO through radiative association is much higher than that of ^{13}CO. Thus, in cold astronomical environments, where carbon monoxide is mainly formed by radiative association, depletion of ^{13}C in CO should be expected[1].

5.2.2 Non-adiabatic couplings

Paper V presents an attempt to go beyond the Born–Oppenheimer approximation in studies of the radiative association process. In this paper

[1]By the time of publication of this thesis the author is not aware of any experimental observation of the isotope effect in radiative association.

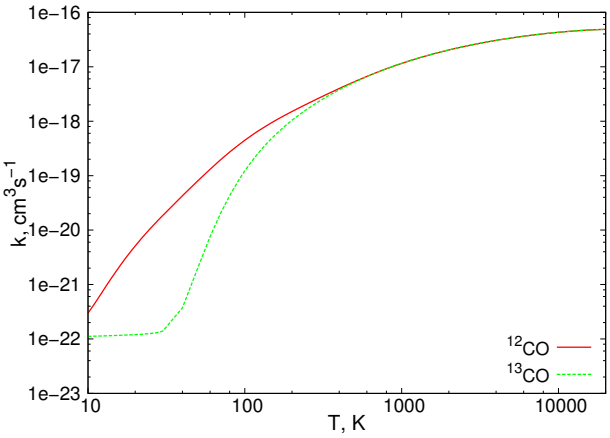

Figure 5.1: Total radiative association rate coefficient for the formation of ^{12}CO and ^{13}CO.

the effects of spin-orbit and rotational couplings on the radiative association of C(^3P) and N(^4S) are investigated. Only couplings between doublet electronic-rotational states of the CN radical are included, which leads to a 6-state model of the process. The main emphasis is placed on the low-energy collisions.

The spin-orbit couplings, the potential energy curves and dipole moments, are obtained using *ab initio* calculations. The CASSCF/MRCI method with full valence active space (9 electrons on 8 orbitals) is used. The rotational couplings are obtained by the transformation of matrix representation of the orbital angular momentum operator ℓ^2 (nuclear rotation) from the Hund's case (e) to Hund's case (a) basis set. The description of the procedure is given in Paper V. The calculation of the cross sections is carried out within the time-independent formalism using the L^2 method with the complex absorbing potential (CAP) as described in Sec. (4.4).

The radiative association cross sections are computed for each of the initial channels (Fig. 5 in Paper V). Careful investigation shows that the channel-specific cross sections have similar patterns in their resonance structures (Fig. 6 in Paper V) and the origin of these is explained.

The total energy-dependent rate coefficient for the process is calculated (Fig. 7 in Paper V). Comparison with the results obtained ignoring the couplings show two main features: an increase of the baseline of the energy-dependent rate coefficient at low collision energies and significant increase in

the number of resonances. The origins of both features are related to the splitting of the asymptotic energy levels in the system caused by the spin-orbit couplings. In general, the observed behavior of the energy-dependent rate coefficient is expected to have a strong influence on the temperature-dependent rate coefficients for the process at low and moderate temperatures.

5.3 Summary

From the results reported in Papers I-IV, an overview of which is presented above, certain conclusions can be made about the formation of diatomic molecules by radiative association. For all considered molecules, the high-energy cross sections have a drop in magnitude, which leads to the decrease of high-temperature rate coefficients. This is caused by the fact that at high collision energies the Franck–Condon (a.k.a vertical) transitions lead to the continuum of the final electronic state rather than to molecule formation in a bound level. Thus, it is expected to be a general feature of the diatomic radiative association.

At low collision energies, when the initial electronic state of approach does not have a potential barrier (as for CN, SiN and SiP) the contribution from the direct (non-resonant) process prevails even at temperatures as low as 10 K and the SC approach provides a good estimate for the rate coefficient of the process. However, this statement applies only to systems which do not include hydrogen atoms. For the hydrogen containing species it was shown that at low temperatures the resonance contribution could be several times higher than the direct one (see e.g. [7, 9, 13]).

The situation is different if the barrier is present on the initial potential (CO). In this case the contribution from the quantum mechanical resonances becomes crucial to get the correct description of the process even at relatively high temperatures (600 K in the case of CO). Moreover, in such situation a pronounced isotope effect in the rate constant can be expected.

Chapter 6

Conclusion and outlook

> Everything is going to be okay
> at the end. If it is not okay, it is
> not the end.
>
> Common believe

Formation of small molecules through radiative association is an astrochemically relevant process, which is actively studied via theoretical simulations. The research presented in this thesis sheds light on some common features of radiative association of some non-hydrogen containing diatoms. The author also hopes that some findings and conclusions drawn from those, which are described in the included papers, contributes to a better understanding of the radiative association process in general.

Despite a considerable progress in simulations of radiative association there are still questions left to be answered even in the case of diatomic systems. Here the author would like to outline what are, in his opinion, the most prominent directions of research in the field of radiative association.

1. Non-adiabatic dynamics
   In Paper V it was shown that the inclusion of non-adiabatic couplings leads to substantial changes in the low-energy part of the radiative association cross section, which in turn should affect the rate coefficient. At present the quantitative effect on the rate constant has not been investigated. Since radiative association can be important at relatively low temperatures, additional study is required.

2. Method development
   As discussed in Paper II a standard approach to the calculation of the radiative association rate coefficient for formation of a diatomic system

is to use the SC method to obtain the direct contribution and account for the resonances through the Breit–Wigner theory. However, the discussed SC method has serious limitations: it can only describe radiative association which involves transition between different electronic states. Also, in the current formulation there is no straightforward generalization of the theory to treat polyatomic systems. Thus, an additional work on the extension of the SC approach is required.[1]

3. Radiative association in polyatomic systems
   As mentioned in Sec. 2.1 radiative association of polyatomic molecules is important in dense molecular clouds and, thus, the rate constants of this process are of interest in astrochemistry. However, even a rigorous quantum mechanical study of triatomic systems is a complicated task and only few calculations exist [14, 16, 24]. Currently, the author is working on radiative association of $H(^2S)$ and $CO(X^1\Sigma^+)$ and some details of the project are given below.

6.1 Towards radiative association of polyatomic molecules: $\mathbf{H(^2S)+CO(X^1\Sigma^+)}$

Calculating the quantum mechanical PT cross section for radiative association requires the bound and scattering wave functions to be computed for each value of the total angular momentum J of the system. In addition, parameters (energies and widths) of the resonances should be obtained in order to estimate their contribution to the rate constant. In the case of triatomic systems each of these tasks can be non-trivial and demands a serious effort. Moreover, accurate potential energy and dipole moments surfaces are necessary in order to get reliable results. The combination of those factors explains why only a few studies of atom-diatom radiative association, which are based on rigorous quantum mechanical treatment, are available in the literature. Moreover, all published work [14, 16, 24] deals with van der Waals complexes and a study on formation of a chemically bound triatomic by radiative association is yet to be seen.

As one of the ongoing projects, the author plans to continue his research on the formation of the HCO radical in its ground electronic state through the following reaction:

$$H(^2S) + CO(X^1\Sigma^+) \rightarrow HCO(X^2A') \rightarrow HCO(X^2A') + h\nu. \qquad (6.1)$$

[1] Certain progress in this area has been achieved recently in our group [57].

Since CO is the second most abundant (after H_2) molecule in the interstellar medium this reaction is of the astrochemical interest.

For the purpose of studying the radiative association of HCO, a new potential energy (PES) and dipole moment surfaces were developed in our group [58]. The *ab initio* calculations were performed with a coupled cluster method with both single and double excitation terms and perturbed triple corrections (CCSD(T)) together with a large diffuse correlation consistent basis set aug-cc-pVQZ. The potential energy surface demonstrates the presence of a high barrier (≈ 0.15 eV) and, thus, quantum mechanical effects are expected to be extremely important in reaction (6.1).

At the present stage, the bound state wavefunctions and corresponding energies have been obtained on new PES. In calculating the bound states the total wavefunction of the system is expanded in the scattering basis:

$$\Psi_{JMv} = \sum_{jl} \frac{1}{R} \psi_{Jvjl}(R) |JMjl\rangle \tag{6.2}$$

where $\psi_{Jvjl}(R)$ are the radial wavefunctions and

$$|JMjl\rangle = \sum_{m_j m_l} \langle JM|jm_j lm_l\rangle |jm_j\rangle |lm_l\rangle$$

are the rotational basis functions. The radial wavefunctions $\psi_{Jvjl}(R)$ are calculated using the renormalized Numerov method as described in Sec. 4.1.2.

Preliminary calculations show that new PES supports at least 4 van der Waals states for $J = 0$, which have not been observed before on other existing potentials. Due to the high barrier, at low temperatures two competing paths would exist for radiative association: tunneling through the barrier and formation of a van der Waals complex. Which of these path plays a dominant role in the process is yet to be seen.

Bibliography

[1] R. C. Dunbar. Polyatomic ion-molecule radiative association: Theoretical framework and predictions: Observations of $NO^+ + C_5H_5CN$ as an example. *Int. J. Mass Spectrom. Ion Processes*, 100:423–443, 1990.

[2] E. Herbst and R. C. Dunbar. A global view of radiative association as a function of product size: interstellar implications. *Mon. Not. R. Atron. Soc.*, 253:341–349, 1991.

[3] J. F. Babb and K. P. Kirby. Molecule Formation in Dust-poor Enviroments. In T. W. Hartquist and D. A. Williams, editors, *The Molecular Astrophysics of Stars and Galaxies*, pages 11 – 34. Clarendon Press, Oxford, 1998.

[4] A. I. Vasyunin, D. Semenov, Th. Henning, V. Wakelam, E. Herbst, and A. M. Sobolev. Chemistry in protoplanetary disks: A sensitivity analysis. *Astrophys. J.*, 672:629–641, 2008.

[5] A. Dalgarno, J. F. Babb, and Y. Sun. Radiative associaiton in planetary atmospheres. *Planet. Space Sci.*, 40:243–246, 1992.

[6] P. C. Stancil and A. Dalgarno. The radiative association of H and D. *Astrophys. J.*, 490:76–78, 1997.

[7] A. S. Dickinson. Radiative associaiton of H and D. *J. Phys. B*, 38:4329–4334, 2005. Corrigendum: J. Phys. B **41** 049801 (2008).

[8] P. D. Singh and C. M. Andreazza. The formation of CN and CN^+ by direct radiative association. *Astrophys. J.*, 537:261–263, 2000.

[9] O. J. Bennett, A. S. Dickinson, T. Leininger, and F. X. Gadéa. Radiative association in Li + H revised: the role of quasi-bound states. *Mon. Not. R. Astron. Soc.*, 341:361–368, 2003. Erratum: Mon. Not. R. Astron. Soc. **384** 1743 (2008).

[10] R. Martinazzo and G. F. Tantardini. Testing wave packet dynamics in computing radiative association cross sections. *J. Chem. Phys.*, 122:094109, 2005.

[11] A. Dalgarno, M. L. Du, and J. H. You. The radiative association of C and O and C^+ and O. *Astrophys. J.*, 349:675–677, 1990.

[12] C. M. Andreazza, R. M. Vichietti, and E. P. Marinho. Formation of SiC by radiative association. *Mon. Not. R. Astron. Soc.*, 400:1892–1896, 2009.

[13] W. P. Kraemer, M. Juřek, and V. Špirko. *Vibrational-Rotational Spectroscopy and Molecular Dynamics*, chapter Quantum-mechanical studies of radiative association reactions: formation of HeH^+, NeH^+ and ArH^+. World Scientific, Singapore, 1997.

[14] F. Mrugała, V. Špirko, and W. P. Kraemer. Radiative association of HeH_2^+. *J. Chem. Phys.*, 118:10547–10560, 2003.

[15] Ǧ. Barinovs and M. C. van Hemert. CH^+ radiative association. *Astrophys. J.*, 636:923–926, 2005.

[16] F. Mrugała and W. P. Kraemer. Radiative association of He^+ with H_2 at temperatures below 100 K. *J. Chem. Phys.*, 122:224321, 2005.

[17] B. Zygelman and A. Dalgarno. The radiative association of He^+ and H. *Astrophys. J.*, 365:239–240, 1990.

[18] D. Gerlich and S. Horning. Experimental Investigation of Radiative Association Processes as Related to Interstellar Chemistry. *Chem. Rev.*, 92:1509–1539, 1992.

[19] D. Gerlich and S. Horning. Ion trap studies of association processes in collisions of CH_3^+ and CD_3^+ with n-H_2, p-H_2, D_2, and He at 80 K. *Astrophys. J.*, 347:849–854, 1989.

[20] S. E. Barlow, G. H. Dunn, and Schauer M. Radiative Association of CH_3^+ and H_2 at 13 K. *Phys. Rev. Lett.*, 52:902–905, 1984.

[21] R. C. Dunbar. Modeling radiative association kinetics. *Int. J. Mass Spectrom. Ion Processes*, 160:1–16, 1997.

[22] S. Petrie and R. C. Dunbar. Radiative association reactions of Na^+, Mg^+, and Al^+ with abundant interstellar molecules. Variational transition state theory calculations. *J. Phys. Chem. A*, 104:4480–4488, 2000.

[23] B. H. Bransden and C. J. Joachain. *Quantum Mechanics*. Pearson Education, second edition, 2000.

[24] M. Ayuoz, R. Lopes, M. Raoult, O. Dulieu, and V. Kokoouline. Formation of H_3^- by radiative association of H_2 and H^- in the interstellar medium. *Phys. Rev. A*, 83:052712, 2011.

[25] J. Franz, M. Gustafsson, and G. Nyman. Formation of carbon monoxide by radiative association: a quantum dynamical study. *Mon. Not. R. Astron. Soc.*, 414:3547–3550, 2011.

[26] I. Baccarelli, L. Andric, T. P. Grozdanov, and R. McCarroll. Comparison of L^2 methods for calculations of radiative association cross sections: Application to collisions of Li with H^+. *J. Chem. Phys.*, 117:3013–3019, 2002.

[27] J. K. G. Watson. Hönl–London factors for multiplet transitions in Hund's case a or b. *J. Mol. Spec.*, 252:5–8, 2008.

[28] A. Hansson and J. K. G. Watson. A comment on Hönl-London factors. *J. Mol. Spec.*, 233:169–173, 2005.

[29] B. Zygelman and A. Dalgarno. Radiative quenching of $He(2^1S)$ induced by collisions with ground-state helium atoms. *Phys. Rev. A*, 38:1877–1884, 1988.

[30] J. S. Cohen and J. N. Bardsley. Calculation of radiative single-charge-transfer cross sections for collsions of He^{2+} with He at low energy. *Phys. Rev. A*, 18:1004–1008, 1978.

[31] M. Kimura, A. Dalgarno, L. Chantranupong, Y. Li, G. Hirsch, and R. J. Buenker. Nonradiative and radiative electron capture in collisions of He^+ ions with C atoms below 1000 eV. *Phys. Rev. A*, 49:2541–2544, 1994.

[32] D. R. Bates. Rate of formation of molecules by radiative association. *Mon. Not. R. Astron. Soc.*, 111:303–314, 1951.

[33] R. A. Bain and J. N. Bardsley. Shape resonances in atom-atom collisions I. Radiative association. *J. Phys. B*, 5:277–285, 1972.

[34] G. Breit and E. Wigner. Capture of Slow Neutrons. *Phys. Rev.*, 49:519–531, 1936.

[35] G. Nyman and H.-G. Yu. Quantum theory of bimolecular chemical reactions. *Rep. Prog. Phys.*, 63:1001–1059, 2000.

[36] J. C. Light, I. P. Hamilton, and J. V. Lill. Generalized discrete variable approximation in quantum mechanics. *J. Chem. Phys.*, 82:1400–1409, 1985.

[37] D. T. Colbert and W. H. Miller. A novel discrete variable representation for quantum mechanical reactive scattering via S-matrix Kohn method. *J. Chem. Phys.*, 86:1982–1991, 1992.

[38] B. R. Johnson. New numerical methods applied to solving the one-dimensional eigenvalue problem. *J. Chem. Phys.*, 67:4086–4093, 1977.

[39] B. R. Johnson. The renormalized Numerov method applied to calculating bound states of the coupled-channel Schrödinger equation. *J. Chem. Phys.*, 69:4678–4688, 1978.

[40] R. G. Gordon. New Method for Constructing Wavefunctions for Bound States and Scattering. *J. Chem. Phys.*, 51:14–25, 1969.

[41] R. N. Zare. *Angular momentum*. A Wiley-Interscience Publication, New York, 1988.

[42] I. N. Bronsgtein and K. A. Semendyayev. *Handbook of mathematics*. Van Nostrand Reinhold, third edition, 1985.

[43] G. A. Korn and T. M. Korn. *Mathematical handbook for scientists and engineers*. McGraw–Hill book company, second edition, 1968.

[44] R. J. Le Roy. LEVEL 8.0: A Computer Program for Solving the Radial Schrödinger Equation for Bound and Quasibound Levels. *University of Waterloo Chemical Physics Research Report CP-663*, 2007.

[45] R. J. Le Roy and L. Wing-Ki. Energies and widths of quasibound levels (orbiting resonances) for spherical potentials. *J. Chem. Phys.*, 69:3622, 1978.

[46] J. N. L. Connor and A. D. Smith. Uniform semiclassical calculation of resonance energies and widths near a barrrier maximum. *Mol. Phys.*, 43:397–414, 1981.

[47] N. Moiseyev. Quantum theory of resonances: calculating energies, widths and cross-sections by complex scaling. *Phys. Rep.*, 302:211–293, 1998.

[48] T. Seideman. A new method for the calculation of photodissociation cross section. *J. Chem. Phys.*, 98:1989–1998, 1992.

[49] H. O Karlsson. Stability of the complex symmetric Lanczos algorithm for computing photodissociation cross sections using smooth exterior scaling or absorbing potentials. *J. Phys. B*, 42:125205, 2009.

[50] S. J. Petuchowski, E. Dwek, Jr. Allen, J. R., and J.A. Nuth. CO formation in the metal-rich ejecta of SN 1987A. *Astrophys. J.*, 342:406–415, 1989.

[51] S. C. O. Glover, C. Federrath, M.-M. Mac Low, and R. S. Klessen. Modelling CO formation in the turbulent interstellar medium. *Mon. Not. R. Astron. Soc.*, 404:2–29, 2010.

[52] R. A. Gearhart, J. C. Wheeler, and D. A. Swartz. Carbon monoxide formation in SN 1987A. *Astrophys. J.*, 410:944–966, 1999.

[53] B. E. Turner. Detection of SiN in IRC+10216. *Astrophys. J.*, 388:L35–L38, 1992.

[54] T. Shilke, S. Leurini, K. M. Menten, and J. Alcolea. Interstellar SiN. *Astron. Astrophys.*, 412:L15–L18, 2003.

[55] P. D. Singh, G. C. Sanzovo, A. C. Borin, and F. R. Ornellas. The radiative association of Si and N atoms, C and O atoms, and C atoms and S^+ ions. *Mon. Not. R. Astron. Soc.*, 303:261–263235, 1999.

[56] C. M. Andreazza, E. P. Marinho, and P. D. Singh. Radiative association of C and P, and Si and P atoms. *Mon. Not. R. Astron. Soc.*, 372:1653–1656, 2006.

[57] M. Gustafsson. Classical calculations of radiative association in absence of electronic transitions. *J. Chem. Phys.*, 138:074308, 2013.

[58] H.-G. Yu, S. V. Antipov, M. Gustafsson, and G. Nyman. The bound states of HCO on a new ab initio based analytic potential energy surface. *In progress.*